Investigating the synergistic potential Si and biochar to immobilize soil Ni in a contaminated calcareous soil after *Zea mays* L. cultivation

Hamid Reza Boostani[1], Ailsa G. Hardie[2], Mahdi Najafi-Ghiri[1], Ehsan Bijanzadeh[3], Dariush Khalili[4], Esmaeil Farrokhnejad[1]

[1]Department of Soil Science, College of agriculture and natural resources of Darab, Shiraz University, Darab74591, Iran.

[2]Department of Soil Science, Faculty of AgriSciences, Stellenbosch University, Private Bag X1, Matieland 7602, South Africa

[3]Department of agroecology, College of agriculture and natural resources of Darab, Shiraz University, Darab 74591, Iran

[4]Department of Chemistry, College of Sciences, Shiraz University, Shiraz 71454, Iran

Correspondence to: Hamid Reza Boostani (hr.boostani@shirazu.ac.ir)

Abstract. Silicon (Si) is a beneficial plant element that has been shown to mitigate the effects of potentially toxic elements (PTEs) on crops. Biochar is a soil amendment that sequesters soil carbon, and that can immobilize PTEs and enhance crop growth in soils. No previous studies have examined the potentially synergistic effect of Si and biochar on soil Ni chemical fractions and immobilization. Therefore, the aim of this study was to examine the interaction effects of Si levels and biochars, to alleviate soil Ni bioavailability and its corresponding uptake in corn (*Zea Mays*) in a calcareous soil. A 90-day factorial greenhouse study with corn was conducted. Si application levels were applied at 0 (S_0), 250 (S_1) and 500 (S_2) mg Si kg^{-1} soil and biochar treatments (3% wt.) including rice husk (RH) and sheep manure (SM) biochars produced at 300°C and 500°C (SM300, SM500, RH300 and RH500). At harvest, corn shoot Ni-concentrations, soil chemical Ni fractions and DPTA-release kinetics were determined. Simultaneous utilization of Si and SM biochars led to a synergistic reduction (15-36%) of soluble and exchangeable soil Ni fractions compared to application of Si (5-9%) and SM (5-7%) biochars separately. The application of the Si and biochars also decreased DPTA-extractable Ni and corn Ni shoot concentration (by up to 57%), with the combined application of SM500+S_2 being the most effective. These effects were attributed to the transformation of Ni from more bioavailable fractions to more stable iron oxide bound fractions, related to soil pH increase. The SM500 was likely the most effective biochar due to its higher alkalinity and lower acidic functional group content which enhanced Ni sorption reactions with Si. The study demonstrates the synergistic potential of Si and sheep manure biochar at immobilizing Ni in contaminated calcareous soils.

1 Introduction

One of the most important ways for potentially toxic elements (PTEs) to enter the human food chain is through the consumption of plants grown in soils contaminated with PTEs. Potentially toxic elements pollute soil environments as a result of mining, metal smelting, using sewage sludge and domestic and industrial effluents in agriculture especially in developing countries (Liu et al., 2018). Potentially toxic elements in soils cannot undergo biodegradation by living organisms, so they possess great stability and longevity in the soil (Poznanović Spahić et al., 2019). Unlike other PTEs found in soils, such as mercury (Hg), cadmium (Cd) and lead (Pb), nickel (Ni) is essential for plant growth at very low concentrations. Nevertheless, at elevated contents (>35 mg Ni kg^{-1} soil), it causes many physiological and morphological malfunctions in plants and severely stunts their growth (Shahzad et al., 2018; Antoniadis et al., 2017). In agricultural soils of Iran in the vicinity of the industrial areas, the weighted average concentration of Ni is 349.8 mg kg^{-1} soil. In these soils, the pollution index (the ratio of the element concentration to the standard concentration) calculated for the Ni is greater than 5, which indicates a severe degree of pollution from the point of view of environmental protection (Shahbazi et al., 2022). Shahbazi et al. (2020) collected 711 agricultural soil samples from different climates of Iran and reported that the Ni content in the soils was between 2.79 mg kg^{-1} and 770 mg kg^{-1} with an average of 68 mg kg^{-1} soil. The results showed that the concentration of Ni in 11.3% of these soils was higher than the threshold value. Removing PTEs from contaminated sites via traditional methods such as pump and treat technologies, soil washing and excavation is very expensive and time-consuming, therefore, for plant cultivation in these areas, low-cost and effective methods should be sought to stabilize PTEs in soils and prevent them from being transferred to the plant (Gao et al., 2023).

Silicon (Si) is a valuable nutrient for plant growth, and it is only considered essential for some plant species such as rice. Applying Si to the soil can enhance plant resistance against biological and non-biological tensions, including physiological stress caused by PTEs in soil (Bhat et al., 2019; Yan et al., 2018). The use of Si to promote plant growth and mitigate PTEs toxicity is becoming increasingly popular in agriculture (Li, 2019; Adrees et al., 2015). The application of Si in soils contaminated with PTEs may reduce PTEs bioavailability by increasing soil pH, increasing the secretion of organic ligands by the roots and forming insoluble compounds with PTEs, and ultimately enhancing plant growth (Bhat et al., 2019; Xiao et al., 2021). The soil pH increase associated with Si application is attributed to the hydrolysis reaction of the silicate anion in soil solution which generates hydroxyl ions (Ma et al. 2021).

Biochar is an organic soil amendment that sequesters soil carbon (C) that has received much attention in recent years to stabilize PTEs in polluted sites (El-Naggar et al., 2018). Biochar is a carbon-rich, porous organic material which is prepared in a limited or no oxygen conditions by pyrolysis of organic wastes, including crop and animal residues, urban waste, wood byproduct (Vickers, 2017; Ankita Rao et al., 2023). The organic surface functional groups of biochar such as carboxylic and phenolic groups provide cation exchange capacity in soils (Tomczyk et al., 2020). Addition of biochar to the soil not only improves the soil chemical and physical properties, but also reduces the bioavailability of PTEs in contaminated soils through some physicochemical processes such as sedimentation, complexation, and electrostatic adsorption (Bandara et al., 2020; Deng et al., 2019; Derakhshan Nejad et al., 2018). The complexation of Ni with oxygen-containing functional groups on biochar surfaces including carboxyl, ether, carbonyl, and hydroxyl, has been identified as a key mechanism for Ni immobilization in soil (Alam et al., 2018; El-Naggar et al., 2018). Electrostatic attraction of Ni by negatively charged functional groups on the surfaces of biochar is another potential mechanism for soil Ni stabilization (Ahmad et al., 2014). Increasing soil pH following the application of biochar also promotes Ni adsorption reactions (Uchimiya et al., 2010). However, the efficiency of biochar prepared from different feedstocks and under different production conditions in stabilizing PTEs in soils can vary significantly (Dey et al., 2023).

Potentially toxic elements in soil can exist in different chemical fractions such as water soluble and exchangeable (WsEx), bound to carbonates (CAR), organic materials (OM), iron and manganese oxides (FeMnOx) and residual (Res) (found in minerals) (Singh et al., 1988). The bioavailability of these forms differs, the WsEx fraction has the highest bioavailability and the Res form is considered unusable by plants. The other chemical fractions of PTEs in soils could be potentially accessible for plant roots depending on soil characteristics such as soil texture, soil pH and soil organic matter content (Kamali et al., 2011; Bharti et al., 2018). The diethylene triamine penta-acetic acid (DTPA) extraction is commonly employed for assessing Ni availability in calcareous soils (Lindsay and Norvell, 1978). However, it is important to acknowledge that this methodology solely assesses Ni availability for plants, while the quantity of released Ni may vary across distinct stages of plant development. Consequently, the examination of alterations in extractable Ni levels over time using the DTPA solution can prove valuable in estimating soil Ni bioavailability. The PTE desorption capacities of soils are anticipated to be contingent upon factors such as soil pH, cation exchange capacity, the specific nature of metal ions, and the source of the metals (Kandpal et al., 2005). Furthermore, the release kinetic parameters can provide insight into the mechanisms of PTEs bonding in soils and their potential risk for leaching into groundwater or surface water (El-Naggar et al., 2021). Therefore, sequential extraction methods and release kinetics models have been employed to assess the efficacy of amendment materials in stabilizing PTEs in contaminated soils. Xiao et al. (2021) found that addition of mineral Si fertilizer to a contaminated paddy soil caused a significant decrease in the Cd and Pb fractions bound to carbonates and iron-manganese oxides while the forms of residual and bound to organic matter increased. In another study, application of cotton residue biochar (1.5 wt. %) to a calcareous soil with a light texture containing different levels of Cd contamination was more efficacious than corn and wheat straw biochars in decreasing the WsEx-Cd and Car-Cd forms and enhancing the Res-Cd form. In addition, application of cotton residue biochar decreased EDTA-extractable Cd by 45–52% compared to the control (Boostani et al., 2023a).

As both biochars and Si are economical and effective soil amendments to reduce plant PTE uptake and stress in contaminated soils, their potential synergistic effect on the immobilization of PTEs in soils should be further investigated. Currently, no previous studies have examined the combined application effects of Si and biochars on the chemical fractions and release kinetics of Ni in calcareous soils. The primary objective of the present study was to elucidate the interaction of biochars and Si levels, to alleviate soil Ni bioavailability and its corresponding accumulation in corn (*Zea Mays* L. 604) plant. Additionally, the study sought to elucidate the underlying soil chemical mechanisms that are likely to be responsible for such effects.

2 Materials and methods

2.1 Soil sampling, characterization and Ni treatment

A composite soil sample from the surface layer (0-30 cm) was collected with an auger at the research farm of the College of Agriculture and Natural Resources in Darab, southern Iran (28° 45′ 0.99″ N 54° 26′ 52.14″ E, Elevation 1105 m). The soil sample was air-dried, sieved through a 2 mm mesh, and then physicochemical properties were determined. Soil sand, silt and clay content were determined by sieving and the hydrometer method (Gee and Bauder, 1986). Soil pH and EC were determined using a saturated paste (Rhoades, 1996), while organic matter was determined using Walkley-Black procedure (Nelson and Sommers, 1996). Calcium carbonate equivalent (CCE) was determined by acid neutralization (Loeppert and Suarez, 1996), while cation exchange capacity was determined using 1M ammonium acetate (Merck, 99%) method (Sumner and Miller, 1996). Available Ni was determined using DPTA (Merck, 99%) extraction (Lindsay and Norvell, 1978). Plastic containers were filled with two kilograms of soil and then 500 mL $NiCl_2$ (Merck, 99%) solution was mixed into to them to achieve a Ni concentration of 300 mg Ni kg^{-1} soil. The Ni-treated soil samples were then allowed to dry out at room temperature, and then rewetted to field capacity using deionized water and allowed to dry out again. The rewetting and room temperature drying cycle was repeated three times to allow the Ni to equilibrate with the soil (Boostani et al., 2023c).

2.2 Production of biochar and its properties

The sheep manure and rice husk were respectively procured from an active animal husbandry and rice mill factory situated in the Darab region, Fars province, Iran. Subsequently, the raw materials underwent a 1-week period of air-drying, followed by electrical milling and sieving through a 2 mm mesh. A slow pyrolysis procedure (2 h at 300 °C and 500 °C) in an oxygen-limited environment was carried out to generate biochars from feedstocks (Anand et al., 2023). The generated biochars were then cooled at ambient temperature and sieved with a 0.5 mm mesh to ensure consistent particle size. The chemical characteristics of the biochars were assessed using the following standard methods. Biochar pH and EC was determined in a 1:10 deionized water suspension (Sun et al., 2014), while CEC was determined using the method of Abdelhafez et al. (2014). Biochar total C, N and H contents was determined by elemental analyzer (ThermoFinnigan Flash EA 1112 Series, Thermoscientific, USA). Biochar moisture and ash content were determined by heating in an oven, while the O+S content was calculated by subtraction of C, N, H, ash and moisture content from total biochar mass (Keiluweit et al., 2010). Biochar total Ni content was determined by combustion and dissolution of the ash in 2M HCl (Merck, 37%) (Boostani et al., 2018a). The Ni content in the acid solution was determine using atomic absorption spectroscopy (AAS) (PG 990, PG Instruments Ltd., UK). The biochar surface functional groups were assessed using Fourier Transform Infrared (FTIR) spectroscopy using a Shimadzu DR-8001 instrument and KBr pellet transmission method. Biochar morphology was assessed using scanning electron microscopy (SEM) (TESCAN-Vega3, Czech Republic).

2.3 Greenhouse experiment

A completely randomized factorial experiment was conducted in a greenhouse environment with three replications. The first factor consisted of the biochar treatments including rice husk (RH) and sheep manure (SM) generated at 300 °C and 500 °C (Control (C) (with no biochar), SM300, SM500, RH300 and RH500), each at the rate of 3%wt. The second factor included Si application levels (0 (S_0), 250 (S_1) and 500 (S_2) mg Si kg^{-1} soil) supplied as Na_2SiO_3 (Sigma Aldrich, 98%) solution. Based on the experimental design, Si levels were added to the 2 kg of Ni-treated soil samples and after drying the soil and mixing it, the prepared biochars were added to the required amount. Immediately after that, the treated soil samples were transferred to plastic pots (45 pieces each containing 2 kg soil) and to facilitate the required reactions, the moisture content of the samples was kept at field capacity level for a duration of two weeks. Thereafter, 6 corn seeds (*Zea mays* L. 604) were planted in each pot, and at the 4-leaf stage, 2 plants were kept in each pot until the end of cultivation. During the growth of the plant, distilled water was used to maintain the soil moisture content in the pots at field capacity. After 90 days, the plants were harvested at the soil interface, rinsed with distilled water to remove contamination, immediately air-dried and kept for Ni determination of plant shoots. After separating the roots and air drying, the soil of the pots was sifted via a 2 mm mesh, and subsequently utilized for performing Ni release kinetics experiment and determining the Ni chemical fractions.

2.4 Sequential extraction procedure

The present study employed a successive extraction technique (Singh et al., 1988) to fractionate soil nickel (Ni) in the following chemical forms, namely water-soluble and exchangeable (WsEx), carbonate-bound (Car), organic matter-bound (OM), manganese oxide-bound (MnOx), amorphous iron oxide-bound (AFeOx), crystalline iron oxide-bound (CFeOx), and residual (Res). The methodological specifics are provided in Table 1.

Table 1
Successive extraction technique of Singh et al. (1988)

Chemical speciation containing Ni	acronym	Duration of agitation (h)	Extractants	Relative density ($g.cm^{-3}$)
Exchangeable and soluble	WsEx	2	1 M magnesium nitrate (Merck, 98%)	1.10
Carbonate	Car	5	1 M sodium acetate (Merck, 99%) (pH=5)	1.04
Organic	OM	0.5	0.7 M sodium hypocholoride (pH=8.5)	1.00
Mn oxide	MnOx	0.5	0.1 M hydroxyl amine hydrochloride (Merck, 98%) (pH=2 by nitric acid (Merck, 65%))	1.00
Amorphous Fe oxides	AFeOx	0.5	0.25 M hydroxyl amine hydrochloride (Merck, 98%) + 0.25 M choloridric acid (Merck, 37%)	1.01
Crystalline Fe oxides	CFeOx	0.5	0.2 M ammonium oxalate (Merck, 99%) + 0.2 M oxalic acid (Merck, 99%) + 0.1 M ascorbic acid (Merck, 99.7%)	1.02

2.5 Release kinetics experiment

A fifty milliliters centrifuge tube was filled with 10 g of soil. After that, 20 ml of DTPA solution (0.005 M DTPA (Merck, 99%) + 0.1 M tri-ethanol amine (Merck, 99%) + 0.01 M calcium chloride (Merck, 97%)) (pH: 7.3) (Lindsay and Norvell, 1978) was added to the soil. The soil-DTPA mixtures were stirred for specific periods of time, i.e. 5, 15, 30, 60, 120, 360, 720 and 1440 minutes at a constant temperature (25 ±2 °C). After each stirring time, the soil suspension was centrifuged (2683 × g) to separate the soil particles from the liquid phase. Atomic absorption spectroscopy (AAS) (PG 990, PG Instruments Ltd., UK) was used to analyze the Ni concentration in the liquid phase. The Ni concentration in the liquid phase versus time was plotted to obtain a Ni release kinetic curve. A total of seven kinetic models namely order models (zero, first, second and third), parabolic diffusion, power function and simple Elovich were assessed to fit the Ni release data. The best models for describing the data were selected according to the maximum value of the coefficient of determination (R^2) and the minimum amount of the standard error of estimate (SEE)(Nasrabadi et al., 2022).

2.6 Data analysis

The ANOVA test was utilized to assess treatments effects in the individual and combined biochar and silicon treatments. Additionally, a comparison of means was conducted using the MSTATC computer program, applying Duncan's test with a significance level of 5%. Figures were generated using Excel 2013 software. Pearson correlation coefficients among parameters in the dataset were determined using SPSS 12.0.

3 Results and Discussion

3.1 Soil characteristics

The soil used in the study prior to experimental treatment, exhibited a sandy loam texture and possessed alkaline properties with significant calcium carbonate content, while not being classified as saline (Table 2). The quantity of soil organic matter was extremely low, a distinct characteristic of soils from arid and semi-arid regions (Okolo et al., 2023) (Table 2). The relatively low levels of clay and organic matter present in the soil contributed to a correspondingly low soil cation exchange capacity (CEC) (Table 2). The soils in Iran mainly originate from calcareous alluvium under xeric, ustic or aridic and mesic, thermic or hyperthermic moisture and temperature regimes, respectively. These soils have varied properties such as calcium carbonate equivalent (1-81%), clay content (1-75%), EC (0.4-49.0 dS m^{-1}), organic matter (0.1-21.5%) and gypsum content (0-91%) (Ghiri et al., 2011). Furthermore, it should be noted that the concentration of available soil Ni extractable by DTPA was very low (Table 2).

Table 2
Certain physicochemical attributes of the soil prior to cultivation.

Sand (%)	58.0
Silt (%)	30.0
Clay (%)	12.0
Soil textural class	Sandy loam
$pH_{(s)}$	7.59
EC (dS m^{-1})	2.60
CCE (%)	55.0
OM (%)	0.50
CEC ($cmol_{(+)}kg^{-1}$)	11.7
Total Ni (mg kg^{-1})	28
Ni-DTPA (mg kg^{-1})	0.39

Notes: EC, electrical conductivity; OM, organic matter; CCE, calcium carbonate equivalent; CEC, cation exchange capacity.

3.2 Chemical characteristics of the biochars

As the pyrolysis temperature rose from 300 °C to 500 °C, the SM biochars demonstrated elevated pH and EC values, with the highest levels observed at the highest temperature (Table 3). The elevated levels of alkali salts, which are reflected in the high ash content (Table 3), are the contributing factor behind this observation in the SM biochars in comparison to the RH biochars. Plant-based biochars commonly exhibit reduced levels of dissolved solids in comparison to animal-based biochars (Sun et al., 2014). The SM300 biochar possessed the highest CEC value of 19.70 cmol+ kg^{-1}. The observed phenomenon may be attributed to the diminution of surface functional groups, namely carboxyl and phenol, at elevated pyrolysis temperatures. These groups are predominantly responsible for facilitating the cation exchange capacity (CEC) of biochars (Tomczyk et al., 2020). As the pyrolysis temperature increased, there was an observed increase in the C content of the biochars, and a corresponding decrease in the content of hydrogen, oxygen, and nitrogen (Table 3). The observed increase in the concentration of C as pyrolysis temperature rises is consistent with a concomitant rise in the degree of carbonization. The observed reduction in the levels of H and O might be attributed to the occurrence of dehydration reactions, decomposition of oxygenated bonds, and the liberation of low molecular weight byproducts rich in H and O, as recently noted by Zhao et al. (2017). Nitrogen compound volatilization explains the diminished N content of the biochars at elevated pyrolysis temperatures. The ratios of H:C and O:C are significant indicators of the aromaticity and polarity of biochars; the lower the ratios the more condensed aromatic C the biochar contains (Chatterjee et al., 2020). The results shown in Table 3 indicated that the H:C and O:C mole ratios showed a gradual decrease as the pyrolysis temperature was increased, which can be interpreted as a sign of improved carbonization of the biochars (Zhao et al., 2017). The Ni content in the biochars derived from rice husk was below detection, whereas a limited quantity of Ni was detected in the biochars produced from sheep manure (Table 3).

Table 3
Some physical and chemical properties of the biochars.

	SM300	SM500	RH300	RH500
pH (1:20)	9.96	11.0	9.0	10.3
EC (1:20) (dS m^{-1})	3.94	4.28	0.84	1.17
CEC ($cmol_+$ kg^{-1})	19.70	18.94	18.94	15.33
C (%)	25.4	31.8	45.0	50.0
H (%)	1.85	0.8	2.28	1.06
N (%)	2.10	1.57	1.30	1.10
Ni (mg kg^{-1})	3.0	15.4	Nd	Nd
Moisture content (%)	1.91	1.82	2.65	2.37
Ash content (%)	53.8	60.0	34.2	44.8
H:C mole ratio	0.87	0.30	0.60	0.25
O+S:C mole ratio	0.44	0.09	0.24	0.01

Notes: SM300, sheep manure biochar generated at 300 ˚C; SM500, sheep manure biochar generated at 500 ˚C; RH300, rice husk biochar produced at 300 ˚C; RH500, rice husk biochar produced at 500 ˚C; CEC, cation exchange capacity; EC, electrical conductivity; Nd, non-detectable.

3.3 FTIR and SEM of the biochars

The FTIR spectra of the SM and RH biochars are shown in Figure 1. The SM and RH biochars produced at 300 °C contained a higher content of carboxyl groups (1700 cm^{-1}) (Keiluweit et al., 2010) than the biochars produced at 500 °C, which is in agreement with the O:C values of the biochars (Table 3). All of the biochars contained absorption bands associated with lignin (1430 cm^{-1}) and cellulose (1030 -1160 cm^{-1}) (Keiluweit et al., 2010). The SM biochar contained more calcite than the RH biochar as indicated by the greater intensity of calcite characteristic peaks at 1432, 875, and 711cm^{-1} (Myszka et al., 2019) in the SM biochars (Fig. 1a). There was also evidence of the presence of Ca oxalate in the SM biochars, indicated by the characteristic peaks at 1618, 780 and 518 cm^{-1} (Maruyama et al., 2023). All the biochars contained silica as indicated by the intense silica absorption peaks at 1100, 800 and 470 cm^{-1} (Zemnukhova et al., 2015).

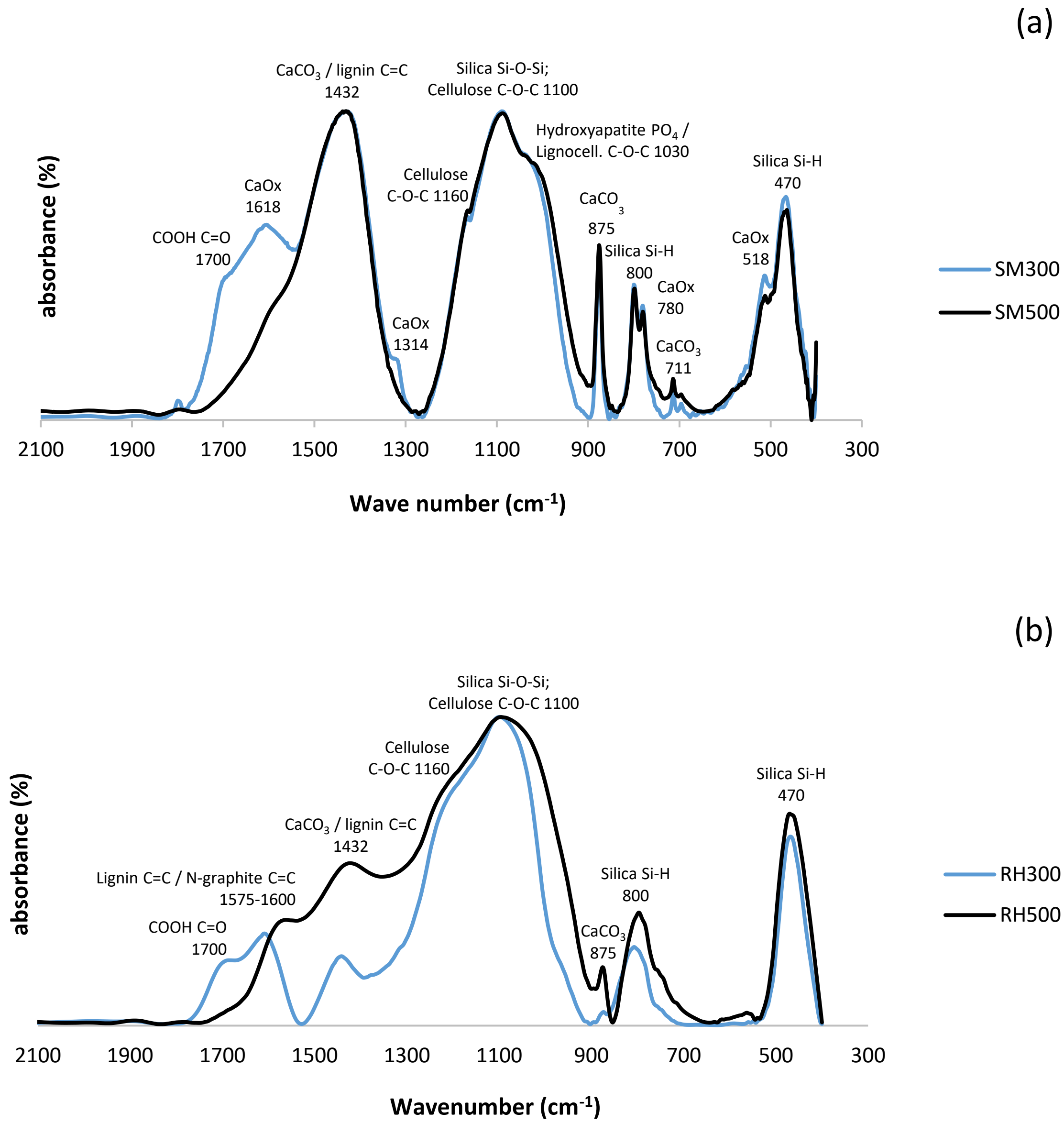

Fig. 1. FTIR of the biochars in the wave number range of 400-2000 cm^{-1}. Notes: SM300, sheep manure biochar produced at 300 ˚C; SM500, sheep manure biochar produced at 500 ˚C; RH300, rice husk biochar produced at 300 ˚C; RH500, rice husk biochar produced at 500 ˚C.

The SEM images of the SM and RH biochars are shown in Figure 2. The morphology of the biochars became more rigid and porous at higher temperatures, as evidenced by the cell wall shrinkage attributed to devolatilization of organic tissues (Claoston et al., 2014).

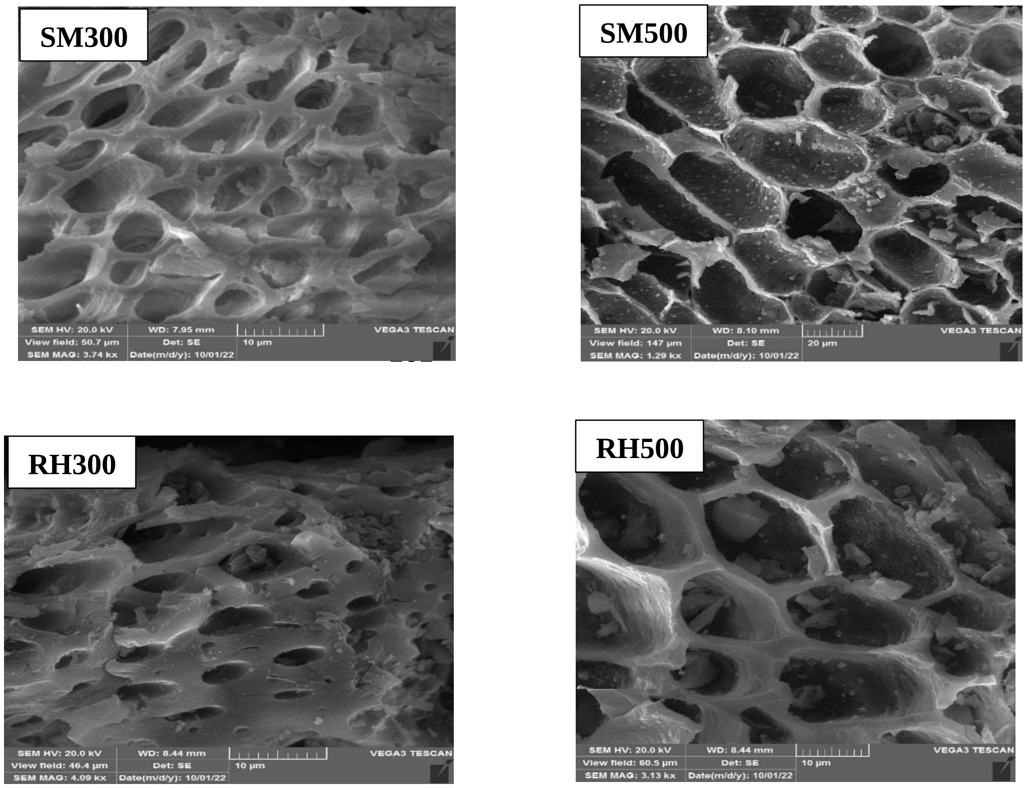

Fig. 2. SEM of the biochars. Notes: SM300, sheep manure biochar produced at 300 ˚C; SM500, sheep manure biochar produced at 500 ˚C; RH300, rice husk biochar produced at 300 ˚C; RH500, rice husk biochar produced at 500 ˚C.

3.4 Soil Ni chemical fractions after the addition of silicon and biochars

The main effects of treatments (biochars and Si levels) and their interactions had a statistically significant effect (P<0.01) on all the soil Ni chemical fractions, except for the Ni-Car fraction, where only the main effects were significant. The soil Ni concentration in the WsEx fraction was significantly reduced by the application of Si rates from S_0 to S_2 by 14.8% (Table 4). Among the biochar treatments, the greatest decrease in WsEx-Ni fraction compared to the control was due to SM500 by 17%, while the RH300 treatment had no significant effect (Table 4). The interaction effect of treatments indicated that the lowest WsEx-Ni concentration was due to the combined treatment of SM500+S_2 (4.04 mg Ni kg^{-1} soil) (Table 4). The combined treatment of S_2 and SM biochars had strong synergistic effect on reducing WsEx-Ni fraction (23-36% reduction) compared to the sum of the treatments alone (13-15% reduction) (Fig. 3). Whereas this synergistic effect of the combined treatments was not evident for the RH biochars (Fig. 3). There was a negative correlation between soil WsEx fraction and soil pH ($r = -0.66, p < 0.01$) indicating that the reduction in WsEx fraction was strongly linked to the increase in soil pH due to the amendments. Previous studies have also shown that application of biochars and silicates result in increases in soil pH, thus reducing the bioavailability of PTEs and their conveyance to plant roots (Shen et al., 2020; Ma et al., 2021). Among the applied biochars, the maximum pH and ash content (Table 3) and calcite (lime) content (Fig. 1) were attributed to the SM500 biochar. Therefore, the combined SM500+S_2 was most effective at reducing WsEx-Ni fraction, likely due to the higher alkalinity and ash content of SM500 promoting Ni precipitation and adsorption (Sachdeva et al., 2023).

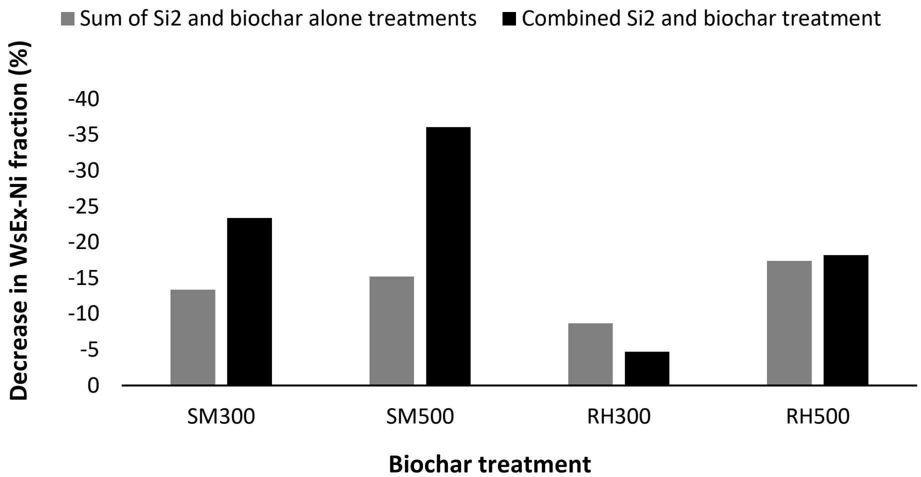

Fig. 3. Comparison of the effect of sum of the Si_2 and biochar alone treatment versus the combined Si_2 and biochar treatments on the % reduction of the WsEx-Ni fraction. Notes: SM300, sheep manure biochar produced at 300 ˚C; SM500, sheep manure biochar produced at 500 ˚C; RH300, rice husk biochar produced at 300 ˚C; RH500, rice husk biochar produced at 500 ˚C.

The reduced effectiveness of biochars produced at 300 °C, as compared to those produced at 500 °C, in decreasing soil Ni-WsEx content could probably be attributed to the lower rates of microbial oxidation and mineralization of RH500 and SM500, which is indicated by their higher environmental stability (as reflected by lower H/C mole ratio values) (Table 3). Consequently, biochar produced at 500 °C may not provide sufficient acidic carboxyl functional groups to the soil to stimulate SOM decomposition, leading to a greater increase in soil pH (Sun et al., 2023). According to Zhu et al. (2015), the addition of wine lees-based biochar (a material from a wine processing factory) to a heavy metal-contaminated soil (at rates of 0.5% and 1% w/w) resulted in an increase in soil pH and a decrease in the soil Ni content in the WsEx fraction. Furthermore, the increase in soil pH due to the increase in Si levels may lead to the precipitation of Ni in the forms of Ni silicate and hydroxide. Due to the high solubility of Na metasilicate, the hydrolysis of silicate anion in the soil solution is intensified, leading to a high concentration of OH^- and a subsequent increase in soil pH (Ma et al., 2021).

Table 4
Effects of biochars and silicon levels on the soil Ni chemical fractions (mg kg^{-1}) and Ni mobility factor (%) after corn cultivation.

	C	SM300	SM500	RH300	RH500	Mean
			WsEx			
S_0	6.32 a	6.02 a-c	5.91 bc	6.31 a	5.77 c	**6.07 A**
S_1	6.03 a-c	5.37 d	5.09 de	6.25 ab	5.28 d	**5.60 B**
S_2	5.77 c	4.84 e	4.04 f	6.02 a-c	5.17 de	**5.17 C**
Mean	**6.04 A**	**5.41 B**	**5.01 C**	**6.20 A**	**5.41 B**	
			OM			
S_0	9.72 a	10.15 a	8.04 d-f	10.08 a	9.02 b	**9.40 A**
S_1	9.60 a	9.75 a	7.16 g	8.62 b-d	8.70 bc	**8.76 B**
S_2	8.11 c-f	7.94 ef	7.12 g	8.30 c-e	7.63 fg	**7.82 C**
Mean	**9.14 A**	**9.28 A**	**7.44 C**	**8.99 A**	**8.44 B**	
			MnOx			
S_0	11.58 a	3.77 kl	5.99 f	4.69gh	9.71 c	**7.15 A**
S_1	10.33 b	3.50 l	5.00 g	4.57 hi	8.93 d	**6.48 B**
S_2	10.28 b	2.98 m	4.28 ij	3.96 jk	7.94 e	**5.89 C**
Mean	**10.73 A**	**3.42 E**	**5.09 C**	**4.41 D**	**8.86 B**	
			AFeOx			
S_0	11.15 ef	10.38 g	11.83 d	10.96 fg	11.75 de	**11.21 C**
S_1	12.20 b-d	10.73 fg	12.03 cd	12.20 b-d	12.66 bc	**11.96 B**
S_2	12.84 b	12.18 b-d	12.16 b-d	12.31 b-d	14.25 a	**12.74 A**
Mean	**12.06 B**	**11.09 C**	**12.00 B**	**11.82 B**	**12.88 A**	
			CFeOx			
S_0	77.32 f	77.98 f	83.97 cd	84.67 cd	79.60 ef	**80.67 C**
S_1	77.89 f	82.20 de	86.34 bc	85.12 b-d	83.62 cd	**83.03 B**
S_2	79.92 ef	85.50 bc	87.88 ab	85.69 bc	90.40 a	**85.88 A**
Mean	**78.37 C**	**81.89 B**	**86.00 A**	**85.16 A**	**84.54 A**	
			Res			
S_0	199.7 c-e	207.5 a	199.8 c-e	196.5 f	197.8 d-f	**200.3 A**
S_1	199.9 c-e	204.5 b	200 cd	197.3 ef	195.5 f	**199.5 A**
S_2	200.3 cd	204.1 b	201 c	199.4 c-e	190.4 g	**199 A**
Mean	**200 B**	**205.4 A**	**200.3 B**	**197.7 B**	**194.6 BC**	

Notes: C, control; SM300, sheep manure biochar produced at 300 ˚C; SM500, sheep manure biochar produced at 500 ˚C; RH300, rice husk biochar produced at 300 ˚C; RH500, rice husk biochar produced at 500 ˚C; S_0, without Si addition; S_1, application of 250 mg Si kg^{-1} soil; S_2, application of 500 mg Si kg^{-1} soil. WsEx, water soluble and exchangeable fraction; OM, organic fraction; MnOx, bound to manganese oxides; AFeOx, bound to amorphous iron oxides; CFeOx, bound to crystalline iron oxides; Res, residual fraction; MF, mobility factor.
*Numbers followed by same letters in each column and rows, in each section, are not significantly ($P<0.05$) different

Application of Si rates from S_0 to S_2 significantly decreased the soil Ni content in the Car fraction by 11.70% (from 15.24 mg Ni kg^{-1} soil to 13.46 mg Ni kg^{-1} soil) (Figure 4). The SM biochars had no significant effect on the Car-Ni fraction whereas addition of RH biochars led to a significant increase in this fraction (Figure 4). Ippolito et al. (2017) found that addition of two biochars (pine [*Pinus contorta*] and tamarisk [*Tamarix* spp.]) to a mine contaminated soil caused a significant increase in the soil Cd content bound to carbonates. They concluded that the reduction in Cd bioavailability may have been due to the ability of biochar to raise soil pH levels and induce the precipitation of $CdCO_3$. Similarly, Yuan et al. (2011) proposed that the decrease in PTEs bioavailability in soil might have been caused by the creation of metal-carbonate species and carbonate-surface functional group reactions, which could function as a mechanism for sequestration. The decrease in the concentration of Ni in the carbonate form with an increase in the Si levels could potentially be explained by the competition between silicate (SiO_4^{-4}) and carbonate ions for binding with Ni^{+2} ions in the soil solution (Sparks et al., 2022).

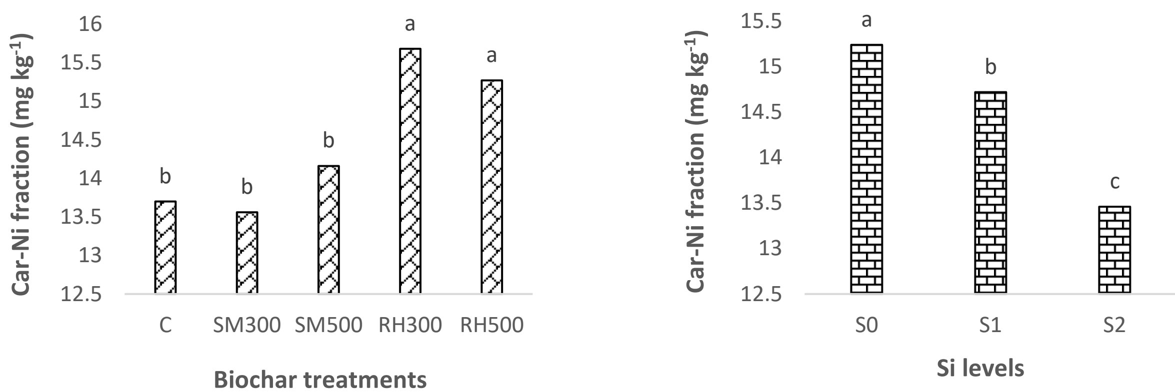

Fig. 4. Effects of (a) biochars and (b) silicon levels on the soil Ni concentration (mg kg^{-1}) in the carbonate-bound fraction after corn cultivation. Notes: C, control; SM300, sheep manure biochar produced at 300 ˚C; SM500, sheep manure biochar produced at 500 ˚C; RH300, rice husk biochar produced at 300 ˚C; RH500, rice husk biochar produced at 500 ˚C; S_0, without Si addition; S_1, application of 250 mg Si kg^{-1} soil; S_2, application of 500 mg Si kg^{-1} soil. * Numbers followed by same letters in each section, are not significantly ($P<0.05$) different.

The biochars produced at 300 °C had no significant effect on the OM-Ni fraction compared to control, while the biochars generated at 500 °C significantly decreased it (Table 4). The greatest OM-Ni reduction (18.6%) was due to SM500. Lu et al. (2017) explored how the application of bamboo and rice straw biochars with varying mesh sizes (0.25 and 1 mm) and at three different rates (0, 1, and 5% w/w) affected the distribution of Cd in a contaminated sandy loam soil, using the BCR (Bureau Communautaire de Référence) sequential extraction method. In contrast to the present study, they reported that the biochars increased the concentration of the Cd-OM fraction as affected, and that this was closely related to the increase in Cd immobilization. In another study, the application of sheep manure biochar produced at 500 °C at the rate of 3% (w/w) to a Cd-contaminated calcareous soil resulted in a significant increase in the OM-Cd fraction, whereas the addition of other biochar treatments (wheat straw, corn straw, rice husk, licorice root pulp) caused a significant decrease in the concentration of Cd in the OM form when compared to the control soil (Boostani et al., 2018b). In the study conducted by Boostani et al. (2018), the reduction in OM-Cd fraction as affected by application of rice husk biochar is in line with our results, however; the increase in soil OM-Cd content with addition of sheep manure biochar is in conflict with the result of the present study. According to the above-mentioned points, it seems that, in addition to the characteristics of biochar and the level of its application (Lu et al., 2017), soil characteristics (calcium carbonate percentage, soil texture, etc.) and the type of heavy metal can also have a substantial role in the binding of PTEs to soil organic matter. By increasing the Si rates from S_0 to S_2, the OM-Ni fraction was reduced by 16.8% (Table 4). It has been shown that the application of Si to cultivated soils resulted in a reduction of soil organic matter content. This implies that Si facilitates the decomposition and accessibility of organic matter to plants (Ma et al., 2021). The interaction effects of biochars and Si levels showed that the lowest OM-Ni concentration was due to the combined treatment of SM500+S_2 (7.12 mg Ni kg^{-1} soil), which was equal to a 26.7% decrease compared to the combined treatment of C+S_0 (9.72 mg Ni kg^{-1} soil) (Table 4).

All the biochar treatments caused a significant decrease in MnOx-Ni fraction compared to control, with the greatest reduction was attributed to the SM300 by 52.6% (Table 4). The lower temperature biochars were more effective than the higher temperature biochars in decreasing the MnOx-Ni fraction (Table 4). In agreement with the present study, Boostani et al. (2023c) observed that biochars produced from cow manure, municipal solid waste and licorice root pulp at lower pyrolysis temperature (300 °C) decreased the soil Ni content in the MnOx fraction to a greater extent than those prepared at higher temperature (600 °C). Hydrophobicity of biochar is decreased with increasing the pyrolysis temperature (Kameyama et al., 2019). At the same soil water content, the water content of soil pores treated with biochars produced at low pyrolysis temperature is higher due to lower absorption of water by the biochars. Therefore, in soils with high soil pore water content and low oxygen conditions, the concentration of MnOx is decreased due to chemical reduction, while concomitantly, the exchangeable and water-soluble Mn concentration are increased (Sparrow and Uren, 2014). Furthermore, increasing the Si concentration from S_0 to S_2 significantly decreased MnOx-Ni by 17.6% (Table 4). The interaction effect of treatments showed that the highest and the lowest MnOx-Ni concentrations were found in the untreated control (11.58 mg Ni kg^{-1} soil) and combined SM300+S_2 (2.98 mg Ni kg^{-1} soil), respectively (Table 4). The concentrations of soil Ni bound to AFeOx and CFeOx were significantly increased by application of Si levels from S_0 to S_2 by 13.6% and 6.5%, respectively (Table 4). Belton et al. (2012) demonstrated that exogenous silicon application resulted in the attachment of silicate to the surface of iron oxide in the form of a polymer. Following the complexation of ferrosilicon, a significant number of negatively charged functional groups, including silanol, were formed. These groups provided numerous adsorption sites for PTEs, ultimately reducing their bioavailability (Belton et al., 2012). In general, all the biochars caused a significant increase in CFeOx-Ni fraction, and there were no significant differences among the SM500, RH300 and RH500 treatments (Table 4). However, the only the RH500 treatment increased the AFeOx-Ni concentration of soil compared to control (Table 4). Among all the biochars, only the SMB300 resulted in a significant increase in the soil Ni concentration in the Res fraction compared to the control (Table 4). The application of Si also did not significantly effect this form (Table 4).

Mailakeba and Bk (2021) studied the addition of kunai grass biochar (0.75%) to a soil with different Ni contamination levels (0, 56, 100, and 180 mg Ni kg^{-1} soil). They found that the application of the grass biochar increased the Res-Ni fraction and reduced the WsEx and OM-Ni fractions. In another study, Boostani et al. (2023c) demonstrated that the application of biochars (cow manure, municipal compost and licorice root pulp each at 3%(w/w)) to a Ni-contaminated soil increased the concentrations of OM-bound and residual Ni fractions, and decreased the concentrations of WsEx, Car, and Fe/Mn oxide-bound Ni fractions. Whereas, Boostani et al. (2023b) found that the application of manure and compost biochars (3% w/w) to Pb-contaminated soil did not significantly affect the Res-Pb fraction but did decrease the WsEx fraction. Therefore, it seems that the effect of biochars on the transformation of soil PTE chemical fractions depends on the raw materials and production conditions of the biochar, the soil application rates, type of PTEs, the degree of soil contamination with PTEs, the selection of sequential extraction procedure and the soil properties (Mailakeba and Bk, 2021; Boostani et al., 2023a, b; Boostani et al., 2021).

In summary, the application of biochars in the present study resulted in the transformation of Ni in the soil from more bioavailable and mobile fractions (WsEx, MnOx, OM) to more stable forms (AFeOx and CFeOx). These changes were particularly evident in the WsEx fraction when SM biochar was applied in conjunction with silicon, indicating that the simultaneous use of these two substances was much more effective than applying them separately.

3.5 Shoot Ni concentration of *Zea mays L.* as affected by treatments

The main effects of biochars, Si rates and their interactions were statistically significant on the shoot Ni concentration of the corn. Addition of Si levels from S_0 to S_2 resulted in 32% decrease in shoot Ni concentration (Table 5). In addition, the shoot Ni concentration was significantly decreased by application of all the biochar treatments compared to the control (with no biochar addition) (Table 5). The interaction effects of treatments showed that the highest and lowest shoot Ni concentration were due to the combined treatments of C+S_0 (10.4 mg Ni kg^{-1} DM) and SM500+S_2 (4.45 mg Ni kg^{-1} DM), respectively (Table 5). The shoot Ni concentration had a significant and positive correlation with the Ni-WsEx fraction ($r = +0.62, P < 0.01$) while there were a significant and negative correlation between the soil pH ($r = -0.60, P < 0.01$) and Ni-CFeOx fraction ($r = -0.50, P < 0.01$). This indicates that the application of Si and biochar can reduce the shoot Ni concentration by increasing soil pH and, as a result, reducing the amount of Ni in the fraction of WsEx and increasing the Ni content attached to crystalline iron oxides. Boostani et al. (2019a) reported the reduction of shoot Ni concentration of spinach **(***Spinacia oleracea* L.) due to the application rice husk and licorice root pulp biochars (2.5% w/w) application in a Ni-contaminated calcareous soil. Additionally, they reported that the biochars produced at 350 °C were more effective at reducing crop Ni uptake and promoting plant growth than the biochars produced at 550 °C. The most significant factors that contribute to the reduction of PTE-uptake by plants in contaminated soils that have been amended with biochars include surface adsorption of heavy metals, increased soil pH, altered redox conditions of PTEs, improved physical and biological properties of the soil, changes in the activity levels of antioxidant enzymes, and a decrease in the transfer of PTEs to the plant shoots (Zeng et al., 2018; Rizwan et al., 2016). Several studies have investigated the effect of Si application on shoot Ni concentration and other heavy metals in various plant species. Khaliq et al. (2016) observed a notable increase Ni concentration and accumulation within the leaf, stem, and roots of cotton after Ni application. Whereas, Si application was observed to induce a significant reduction in Ni concentrations across these respective plant components. In another study, Maryam et al. (2024) concluded that addition of Si caused an increase in the growth indices of maze through reducing the Pb-shoot concentration. One possible explanation for the reduction in shoot Ni concentration is that Si can compete with Ni for uptake by plant roots. Silicon has a similar ionic radius to Ni, which means that it can occupy the same binding sites on root cell membranes and reduce the uptake of Ni. Additionally, Si can induce the expression of genes that are involved in Ni transport and homeostasis, which may contribute to the reduced shoot Ni concentration (Hossain et al., 2012; Liang et al., 2005).

Table 5
Shoot Ni concentration (mg Ni kg^{-1} DM) as affected by biochars and silicon application levels.

	C	SM300	SM500	RH300	RH500	
S_0	10.4 a	7.35 bc	9.85 a	7.55 bc	7.65 b	**8.56 A**
S_1	7.65 b	6.90 bc	6.60 cd	7.05 bc	7.35 bc	**7.11 B**
S_2	7.20 bc	5.05 ef	4.45 f	5.80 de	6.60 cd	**5.82 C**
Mean	**8.41 A**	**6.43 C**	**6.96 BC**	**6.80 BC**	**7.20 B**	

Notes: C, control; SM300, sheep manure biochar generated at 300 ˚C; SM500, sheep manure biochar generated at 500 ˚C; RH300, rice husk biochar produced at 300 ˚C; RH500, rice husk biochar produced at 500 ˚C; S_0, without Si application; S_1, addition of 250 mg Si kg^{-1} soil; S_2, addition of 500 mg Si kg^{-1} soil. Numbers followed by same letters in each section, are not significantly (P<0.05) different.

3.6 Soil Ni desorption as affected by Silicon levels and biochars

The cumulative soil Ni desorption (extracted by DTPA) as a function of time are shown in Fig. 5. The release of Ni from the soil initially proceeded at a much higher rate during the first hour, and then proceeded at a much slower rate during the next 24 hours, as illustrated by the trend-line in Fig. 5. This two-stage process of releasing heavy metals from soil has also been reported by other researchers (Sajadi Tabar and Jalali, 2013; Boostani et al., 2023a). It is likely that the first stage of release is related to forms of Ni that are less strongly attached to soil particles, including WsEx and Car, while the second stage of desorption is likely from fractions of Ni with less bioavailability, such as FeOx and Res (Saffari et al., 2015). In general, the amount of soil Ni desorption was reduced by addition of biochars and Si levels (Fig. 5). In addition, the effects of biochars produced at higher pyrolysis temperature (500 °C) on reducing the soil Ni release was more than those generated at lower pyrolysis temperature (300 °C). The highest amount of soil Ni release was due to the combined treatment of C+S_0 (37.84 mg Ni kg^{-1} soil) while the lowest was observed in the combined application of SM500 and S_2 (31.13 mg Ni kg^{-1} soil) treatment.

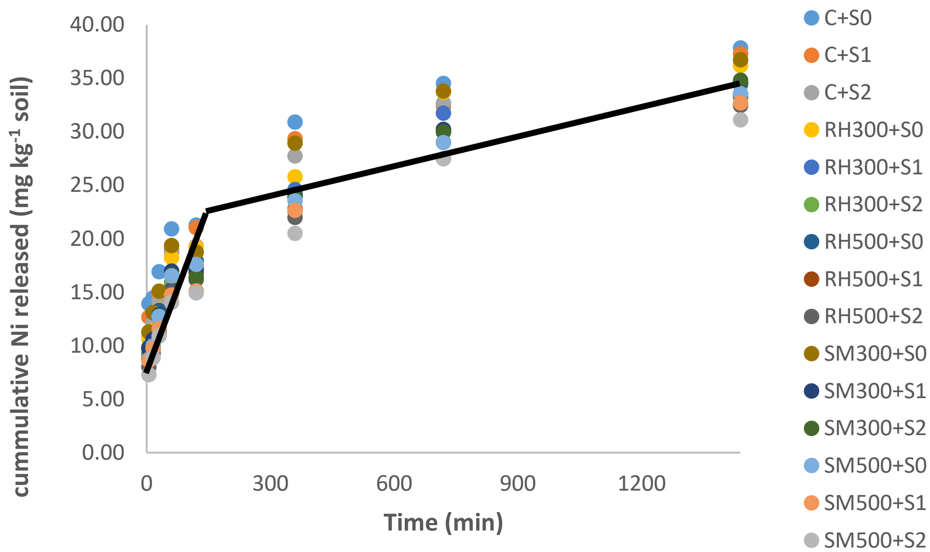

Fig. 5. Cumulative soil Ni desorption (extracted by DTPA) (mg kg^{-1}) as affected by different treatments. Notes: C, control; SM300, sheep manure biochar produced at 300˚C; SM500, sheep manure biochar produced at 500˚C; RH300, rice husk biochar produced at 300˚C; RH500, rice husk biochar produced at 500˚C; S_0, without Si addition; S_1, application of 250 mg Si kg^{-1} soil; S_2, application of 500 mg Si kg^{-1} soil.

3.7 Fitting of Ni release data to kinetics models

The soil Ni release data during 24 hours for all the biochar and Si treatments were evaluated by seven different kinetic models (Table 6). The effectiveness of the various kinetic models to describe the observed soil Ni desorption was analyzed by considering the coefficient of determination (R^2) and standard error of estimate (SEE), so that the highest value of the R^2 and the lowest value of the SEE were set as the criteria. As seen in Table 6, the order kinetic models did not adequately describe soil Ni release, and with the increase in the order of the kinetic model (from zero to third), the value of the R^2 decreased. This has also been found by other researchers for the release of heavy metals from soil (Boostani et al., 2019b; Ghasemi-Fasaei et al., 2006). Whereas, the non-order kinetic models, including power function, parabolic diffusion and simple Elovich, acceptably described the soil Ni release of the various treatments (Table 6). Among them, the power function model was the best according to the highest value of R^2 (0.98) and the lowest value of SEE (0.055). Boostani et al. (2018b) also reported that the power function was the best kinetic model to describe soil Cd desorption from a Cd-contaminated soil treated with biochars and zeolite.

Table 6
The range of coefficients of determination (R^2) and standard error of estimate (SEE) of applied kinetic models to all the soil treatments.

	R^2		SEE	
Kinetic models	Range	Mean	Range	Mean
Zero order	0.79-0.87	0.80	3.36-4.67	3.67
First order	0.69-0.75	0.75	0.22-0.29	0.25
Second order	0.53-0.61	0.52	0.011-0.026	0.0018
Third order	0.39-0.51	0.41	0.0013-0.0052	0.0030
Parabolic diffusion	0.94-0.98	0.96	1.26-2.44	1.85
Power function	0.97-0.99	0.98	0.054-0.057	0.055
Simple Elovich	0.92-0.97	0.95	2.04-2.78	2.50

3.8 Using the parameters of power function model to investigate the effect of treatments on soil Ni desorption

As the power function model ($q = at^b$) described the soil Ni release data the best, its parameters (a and b) were used to investigate the effect of biochar application and Si levels on the release of Ni from the Ni-contaminated soil (Table 7). The main effects of biochars and Si levels and their interactions on the ʽaʼ and ʽbʼ parameters were significant ($P < 0.01$). As Dang et al. (1994) reported, in this kinetics model, a decrease in parameter ʽaʼ and an increase in parameter ʽbʼ indicates a decrease in the rate of heavy metals desorption from the soil. The main effects of treatments showed that addition of all the biochar treatments caused a significant decrease in the ʽaʼ parameter compared to the control while the ʽbʼ parameter was significantly increased (Table 7). The same trend was observed for all the Si treatment rates (Table 7). Therefore, it can be concluded that the use of all the biochars and Si levels has caused a decrease in the rate of Ni release from the Ni-contaminated soil. Generally, there was a greater decrease in Ni desorption in biochar treatments prepared at the higher temperature (Table 7). The interaction effects indicated that the most effective combined treatment in reducing the rate of Ni release from the soil was SM500+S_2 which had the lowest value of parameter ʽaʼ (4.52) and the highest value of parameter ʽbʼ (0.264) among the treatments.

If it is differentiated from the power function equation ($q = at^b$) with respect to time (t) ($dq/dt = ab\ t^{b-1}$), when t = 1 s = 0, the ratio of *dq/dt* becomes ʽ*ab*ʼ. This parameter indicates the amount of heavy metal desorption in the initial time (Dalal, 1985). The ʽ*ab*ʼ parameter was affected by the application of Si levels and biochars, so that this parameter was significantly decreased compared to the control with addition of all the biochars (12.4%, 24.2%, 15.4% and 21.3% for the SM300, SM500, RH300 and RH500, respectively) and Si rates (13% from S_0 to S_2), (Table 7). This finding also confirmed the effect of applied treatments in reducing the amount of Ni release. The greatest reduction was observed in the combined treatment of SM500+S_2 by 33.5% compared to the control (Table 7).

Table 7
The coefficients of power function model as affected by biochars and silicon levels in a Ni-polluted calcareous soil after corn cultivation.

	C	SM300	SM500	RH300	RH500	
			a (mg Ni kg^{-1} h^{-1})[b]			
S_0	9.15 a	7.39 c	5.56 gh	6.49 e	5.95 f	**6.91 A**
S_1	7.92 b	6.01 f	5.23 i	5.66 g	5.21 i	**6.00 B**
S_2	6.90 d	5.39 hi	4.52 k	5.22 i	4.84 j	**5.38 C**
Mean	**7.99 A**	**6.27 B**	**5.11 E**	**5.80 C**	**5.34 D**	
			b (mg Ni $kg^{-1})^{-1}$			
S_0	0.196 i	0.222 g	0.247 d	0.238 e	0.237 e	**0.228 C**
S_1	0.212 h	0.238 e	0.246 d	0.250 cd	0.254 bc	**0.240 B**
S_2	0.230 f	0.254 bc	0.264 a	0.256 b	0.262 a	**0.253 A**
Mean	**0.212 E**	**0.238 D**	**0.252 A**	**0.248 B**	**0.251 AB**	
			ab			
S_0	1.79 a	1.68 c	1.37 h	1.54 e	1.41 g	**1.55 A**
S_1	1.69 b	1.43 f	1.29 k	1.41 fg	1.32 j	**1.42 B**
S_2	1.59 d	1.37 h	1.19 m	1.34 i	1.27 l	**1.35 C**
Mean	**1.69 A**	**1.48 B**	**1.28 E**	**1.43 C**	**1.33 D**	

Notes: C, control; SM300, sheep manure biochar produced at 300 ˚C; SM500, sheep manure biochar produced at 500 ˚C; RH300, rice husk biochar produced at 300 ˚C; RH500, rice husk biochar produced at 500 ˚C; S_0, without Si addition; S_1, application of 250 mg Si kg^{-1} soil; S_2, application of 500 mg Si kg^{-1} soil.
* Numbers followed by same letters in each column and rows, in each section, are not significantly ($P<0.05$) different

The correlation between the parameters of the fitted power function model with soil Ni-chemical fractions, shoot Ni content and soil pH are shown in Table 8. The ʿaʾ and ʿ*ab*ʾ parameters had a positive correlation with the soil WsEx, OM and MnOx Ni fractions, while there was a negative correlation among the ʿaʾ and ʿ*ab*ʾ parameters the AFeOx and CFeOx Ni fractions. This trend was inverse for the ʿbʾ parameter of the power function model. These correlations verified that the application of silicon and biochar to the Ni-contaminated calcareous soil led to a decrease in the rate and amount of Ni release from the soil by reducing the Ni concentration in chemical forms with higher bioavailability including WsEx, OM and MnOx. Furthermore, the ʿaʾ and ʿ*ab*ʾ parameters were negatively correlated with soil pH. Whereas there were positive correlations between these parameters and shoot Ni concentration (Table 8). These findings once again confirmed that the increase in soil pH due to the application of silicon and biochar can cause a decrease in the bioavailability of soil Ni and, as a result, a decrease in the concentration of Ni in aerial parts of the plant.

Table 8
The correlation coefficients (r) between the power function model parameters (a, b, ab) and soil Ni chemical fractions, shoot Ni concentration and soil pH.

	WsEx	Car	OM	MnOx	AFeOx	CFeOx	Res	Shoot Ni Concentration	Soil pH
a	0.63^{**}	0.02^{ns}	0.70^{**}	0.53^{**}	-0.44^{**}	-0.80^{**}	0.27^{ns}	0.62^{**}	-0.52^{**}
b	-0.59^{**}	0.03^{ns}	-0.68^{**}	-0.54^{**}	0.46^{**}	0.83^{**}	-0.28^{ns}	-0.63^{**}	0.51^{**}
ab	0.68^{**}	0.04^{ns}	0.74^{**}	0.46^{**}	-0.46^{**}	-0.80^{**}	0.29^{ns}	0.06^{**}	-0.51^{**}

Notes: WsEx, water soluble and exchangeable fraction; OM, organic fraction; MnOx, bound to manganese oxides; AFeOx, bound to amorphous iron oxides; CFeOx, bound to crystalline iron oxides; Res, residual fraction.
** and ^{ns} indicate significance at the 0.01 probability level and non-significant, respectively.

4 Conclusions

The application of biochars and Si in the present study resulted in the transformation of Ni in the soil from more bioavailable and mobile fractions (WsEx, MnOx, OM) to more stable forms (AFeOx and CFeOx). These changes were particularly evident in the WsEx fraction when SM biochars were applied in conjunction with silicon, indicating a strong synergistic effect related to soil pH increase. Application of all biochars and Si reduced DPTA-extractable Ni release from the soil, which was most strongly associated with the increase in CFeOx fraction. Application of all biochars and Si decreased corn Ni uptake, with the combined SM500+S_2 being the most effective. The decrease in corn uptake was correlated with the decrease in the WsEx-Ni fraction and increase in CFeOx fraction. SM500 was likely the most effective biochar due to its higher alkalinity and ash content, and lower acidic functional group content which enhanced Ni sorption reactions with Si. Future research is needed to better understand the mechanisms underlying the interaction effects of Si and biochar application on the distribution of soil Ni chemical forms and to optimize Si application strategies for sustainable Ni management in agricultural and natural ecosystems.

Authors' Contributions H.R.B. Conceptualization, Formal analysis, Methodology, Investigation, Validation A.G.H. Writing - Review & Editing M.N. Project administration, Visualization E.B. Review & Editing E.F. Laboratory analyses.

Financial support. No funding was received for conducting this study.

Competing interests. The contact author has declared that neither they nor their co-authors have any competing interests.

Data availability. The data generated in this study are available from the corresponding authors upon reasonable request.

Disclaimer. Publisher's note: Copernicus Publications remains neutral with regard to jurisdictional claims in published maps and institutional affiliations.

Acknowledgements: This work was supported by College of Agriculture and Natural Resources of Darab, Shiraz University, Darab, Iran.

References

Abdelhafez, A. A., Li, J., and Abbas, M. H.: Feasibility of biochar manufactured from organic wastes on the stabilization of heavy metals in a metal smelter contaminated soil, Chemosphere, 117, 66-71, 2014.

Adrees, M., Ali, S., Rizwan, M., Zia-ur-Rehman, M., Ibrahim, M., Abbas, F., Farid, M., Qayyum, M. F., and Irshad, M. K.: Mechanisms of silicon-mediated alleviation of heavy metal toxicity in plants: a review, Ecotoxicology and Environmental Safety, 119, 186-197, 2015.

Ahmad, M., Rajapaksha, A. U., Lim, J. E., Zhang, M., Bolan, N., Mohan, D., Vithanage, M., Lee, S. S., and Ok, Y. S.: Biochar as a sorbent for contaminant management in soil and water: a review, Chemosphere, 99, 19-33, 2014.

Alam, M. S., Gorman-Lewis, D., Chen, N., Flynn, S. L., Ok, Y. S., Konhauser, K. O., and Alessi, D. S.: Thermodynamic analysis of nickel (II) and zinc (II) adsorption to biochar, Environmental science & technology, 52, 6246-6255, 2018.

Anand, A., Gautam, S., and Ram, L. C.: Feedstock and pyrolysis conditions affect suitability of biochar for various sustainable energy and environmental applications, Journal of Analytical and Applied Pyrolysis, 170, 105881, 2023.

Ankita Rao, K., Nair, V., Divyashri, G., Krishna Murthy, T., Dey, P., Samrat, K., Chandraprabha, M., and Hari Krishna, R.: Role of Lignocellulosic Waste in Biochar Production for Adsorptive Removal of Pollutants from Wastewater, in: Advanced and Innovative Approaches of Environmental Biotechnology in Industrial Wastewater Treatment, Springer, 221-238, 2023.

Antoniadis, V., Levizou, E., Shaheen, S. M., Ok, Y. S., Sebastian, A., Baum, C., Prasad, M. N., Wenzel, W. W., and Rinklebe, J.: Trace elements in the soil-plant interface: Phytoavailability, translocation, and phytoremediation–A review, Earth-Science Reviews, 171, 621-645, 2017.

Bandara, T., Franks, A., Xu, J., Bolan, N., Wang, H., and Tang, C.: Chemical and biological immobilization mechanisms of potentially toxic elements in biochar-amended soils, Critical Reviews in Environmental Science and Technology, 50, 903-978, 2020.

Belton, D. J., Deschaume, O., and Perry, C. C.: An overview of the fundamentals of the chemistry of silica with relevance to biosilicification and technological advances, The FEBS journal, 279, 1710-1720, 2012.

Bharti, K. P., Pradhan, A. K., Singh, M., Beura, K., Behera, S. K., and Paul, S. C.: Effect of mycorrhizal co-Inoculation with selected rhizobacteria on soil zinc dynamics, International Journal of Current Microbiology and Applied Sciences, 7, 1961-1970, 2018.

Bhat, J. A., Shivaraj, S., Singh, P., Navadagi, D. B., Tripathi, D. K., Dash, P. K., Solanke, A. U., Sonah, H., and Deshmukh, R.: Role of silicon in mitigation of heavy metal stresses in crop plants, Plants, 8, 71, 2019.

Boostani, H., Hardie, A., Najafi-Ghiri, M., and Khalili, D.: Investigation of cadmium immobilization in a contaminated calcareous soil as influenced by biochars and natural zeolite application, International journal of environmental science and technology, 15, 2433-2446, 2018a.

Boostani, H., Hardie, A., Najafi-Ghiri, M., and Khalili, D.: Investigation of cadmium immobilization in a contaminated calcareous soil as influenced by biochars and natural zeolite application, International Journal of Environmental Science and Technology, 15, 2433-2446, 2018b.

Boostani, H. R., Hardie, A. G., and Najafi-Ghiri, M.: Chemical fractions, mobility and release kinetics of Cadmium in a light-textured calcareous soil as affected by crop residue biochars and Cd-contamination levels, Chemistry and Ecology, 1-14, 2023a.

Boostani, H. R., HARDIE, A. G., and NAJAFI-GHIRI, M.: Lead stabilization in a polluted calcareous soil using cost-effective biochar and zeolite amendments after spinach cultivation, Pedosphere, 33, 321-330, 2023b.

Boostani, H. R., Najafi-Ghiri, M., and Mirsoleimani, A.: The effect of biochars application on reducing the toxic effects of nickel and growth indices of spinach (Spinacia oleracea L.) in a calcareous soil, Environmental Science and Pollution Research, 26, 1751-1760, 2019a.

Boostani, H. R., Hardie, A. G., Najafi-Ghiri, M., and Khalili, D.: The effect of soil moisture regime and biochar application on lead (Pb) stabilization in a contaminated soil, Ecotoxicology and Environmental Safety, 208, 111626, 2021.

Boostani, H. R., Hardie, A. G., Najafi-Ghiri, M., and Zare, M.: Chemical speciation and release kinetics of Ni in a Ni-contaminated calcareous soil as affected by organic waste biochars and soil moisture regime, Environmental Geochemistry and Health, 45, 199-213, 2023c.

Boostani, H. R., Najafi-Ghiri, M., Amin, H., and Mirsoleimani, A.: Zinc desorption kinetics from some calcareous soils of orange (Citrus sinensis L.) orchards, southern Iran, Soil science and plant nutrition, 65, 20-27, 2019b.

Chatterjee, R., Sajjadi, B., Chen, W.-Y., Mattern, D. L., Hammer, N., Raman, V., and Dorris, A.: Effect of pyrolysis temperature on physicochemical properties and acoustic-based amination of biochar for efficient CO2 adsorption, Frontiers in Energy Research, 8, 85, 2020.

Claoston, N., Samsuri, A., Ahmad Husni, M., and Mohd Amran, M.: Effects of pyrolysis temperature on the physicochemical properties of empty fruit bunch and rice husk biochars, Waste Management & Research, 32, 331-339, 2014.

Dalal, R.: Comparative prediction of yield response and phosphorus uptake from soil using anion-and cation-anion-exchange resins, Soil Science, 139, 227-231, 1985.

Dang, Y., Dalal, R., Edwards, D., and Tiller, K.: Kinetics of zinc desorption from Vertisols, Soil Science Society of America Journal, 58, 1392-1399, 1994.
Deng, Y., Huang, S., Laird, D. A., Wang, X., and Meng, Z.: Adsorption behaviour and mechanisms of cadmium and nickel on rice straw biochars in single-and binary-metal systems, Chemosphere, 218, 308-318, 2019.
Derakhshan Nejad, Z., Jung, M. C., and Kim, K.-H.: Remediation of soils contaminated with heavy metals with an emphasis on immobilization technology, Environmental geochemistry and health, 40, 927-953, 2018.
Dey, D., Sarangi, D., and Mondal, P.: Biochar: Porous Carbon Material, Its Role to Maintain Sustainable Environment, in: Handbook of Porous Carbon Materials, Springer, 595-621, 2023.
El-Naggar, A., Rajapaksha, A. U., Shaheen, S. M., Rinklebe, J., and Ok, Y. S.: Potential of biochar to immobilize nickel in contaminated soils, in: Nickel in Soils and Plants, CRC Press, 293-318, 2018.
El-Naggar, A., Chang, S. X., Cai, Y., Lee, Y. H., Wang, J., Wang, S.-L., Ryu, C., Rinklebe, J., and Ok, Y. S.: Mechanistic insights into the (im) mobilization of arsenic, cadmium, lead, and zinc in a multi-contaminated soil treated with different biochars, Environment International, 156, 106638, 2021.
Gao, W., He, W., Zhang, J., Chen, Y., Zhang, Z., Yang, Y., and He, Z.: Effects of biochar-based materials on nickel adsorption and bioavailability in soil, Scientific Reports, 13, 5880, 2023.
Gee, G. W. and Bauder, J. W.: Particle-size analysis, Methods of soil analysis: Part 1 Physical and mineralogical methods, 5, 383-411, 1986.
Ghasemi-Fasaei, R., Maftoun, M., Ronaghi, A., Karimian, N., Yasrebi, J., Assad, M., and Ippolito, J.: Kinetics of copper desorption from highly calcareous soils, Communications in Soil Science and Plant Analysis, 37, 797-809, 2006.
Ghiri, M. N., Abtahi, A., Owliaie, H., Hashemi, S. S., and Koohkan, H.: Factors affecting potassium pools distribution in calcareous soils of southern Iran, Arid land research and management, 25, 313-327, 2011.
Hossain, M. A., Piyatida, P., da Silva, J. A. T., and Fujita, M.: Molecular mechanism of heavy metal toxicity and tolerance in plants: central role of glutathione in detoxification of reactive oxygen species and methylglyoxal and in heavy metal chelation, Journal of botany, 2012, 2012.
Ippolito, J., Berry, C., Strawn, D., Novak, J., Levine, J., and Harley, A.: Biochars reduce mine land soil bioavailable metals, Journal of environmental quality, 46, 411-419, 2017.
Kamali, S., Ronaghi, A., and Karimian, N.: Soil zinc transformations as affected by applied zinc and organic materials, Communications in soil science and plant analysis, 42, 1038-1049, 2011.
Kameyama, K., Miyamoto, T., and Iwata, Y.: The preliminary study of water-retention related properties of biochar produced from various feedstock at different pyrolysis temperatures, Materials, 12, 1732, 2019.
Kandpal, G., Srivastava, P., and Ram, B.: Kinetics of desorption of heavy metals from polluted soils: Influence of soil type and metal source, Water, Air, and Soil Pollution, 161, 353-363, 2005.
Keiluweit, M., Nico, P. S., Johnson, M. G., and Kleber, M.: Dynamic molecular structure of plant biomass-derived black carbon (biochar), Environmental science & technology, 44, 1247-1253, 2010.
Khaliq, A., Ali, S., Hameed, A., Farooq, M. A., Farid, M., Shakoor, M. B., Mahmood, K., Ishaque, W., and Rizwan, M.: Silicon alleviates nickel toxicity in cotton seedlings through enhancing growth, photosynthesis, and suppressing Ni uptake and oxidative stress, Archives of Agronomy and Soil Science, 62, 633-647, 2016.
Li, X.: Technical solutions for the safe utilization of heavy metal-contaminated farmland in China: a critical review, Land Degradation & Development, 30, 1773-1784, 2019.
Liang, Y., Wong, J., and Wei, L.: Silicon-mediated enhancement of cadmium tolerance in maize (Zea mays L.) grown in cadmium contaminated soil, Chemosphere, 58, 475-483, 2005.
Lindsay, W. L. and Norvell, W.: Development of a DTPA soil test for zinc, iron, manganese, and copper, Soil science society of America journal, 42, 421-428, 1978.

Liu, L., Guo, X., Wang, S., Li, L., Zeng, Y., and Liu, G.: Effects of wood vinegar on properties and mechanism of heavy metal competitive adsorption on secondary fermentation based composts, Ecotoxicology and environmental safety, 150, 270-279, 2018.

Loeppert, R. H. and Suarez, D. L.: Carbonate and gypsum, Methods of soil analysis: Part 3 chemical methods, 5, 437-474, 1996.

Lu, K., Yang, X., Gielen, G., Bolan, N., Ok, Y. S., Niazi, N. K., Xu, S., Yuan, G., Chen, X., and Zhang, X.: Effect of bamboo and rice straw biochars on the mobility and redistribution of heavy metals (Cd, Cu, Pb and Zn) in contaminated soil, Journal of environmental management, 186, 285-292, 2017.

Ma, C., Ci, K., Zhu, J., Sun, Z., Liu, Z., Li, X., Zhu, Y., Tang, C., Wang, P., and Liu, Z.: Impacts of exogenous mineral silicon on cadmium migration and transformation in the soil-rice system and on soil health, Science of the Total Environment, 759, 143501, 2021.

Mailakeba, C. D. and BK, R. R.: Biochar application alters soil Ni fractions and phytotoxicity of Ni to pakchoi (Brassica rapa L. ssp. chinensis L.) plants, Environmental Technology & Innovation, 23, 101751, 2021.

Maruyama, M., Sawada, K. P., Tanaka, Y., Okada, A., Momma, K., Nakamura, M., Mori, R., Furukawa, Y., Sugiura, Y., and Tajiri, R.: Quantitative analysis of calcium oxalate monohydrate and dihydrate for elucidating the formation mechanism of calcium oxalate kidney stones, Plos one, 18, e0282743, 2023.

Maryam, H., Abbasi, G. H., Waseem, M., Ahmed, T., and Rizwan, M.: Preparation and characterization of green silicon nanoparticles and their effects on growth and lead (Pb) accumulation in maize (Zea mays L.), Environmental Pollution, 123691, 2024.

Myszka, B., Schüßler, M., Hurle, K., Demmert, B., Detsch, R., Boccaccini, A. R., and Wolf, S. E.: Phase-specific bioactivity and altered Ostwald ripening pathways of calcium carbonate polymorphs in simulated body fluid, RSC advances, 9, 18232-18244, 2019.

Nasrabadi, M., Omid, M. H., and Mazdeh, A. M.: Experimental Study of Flow Turbulence Effect on Cadmium Desorption Kinetics from Riverbed Sands, Environmental Processes, 9, 10, 2022.

Nelson, D. W. and Sommers, L. E.: Total carbon, organic carbon, and organic matter, Methods of soil analysis: Part 3 Chemical methods, 5, 961-1010, 1996.

Okolo, C. C., Gebresamuel, G., Zenebe, A., Haile, M., Orji, J. E., Okebalama, C. B., Eze, C. E., Eze, E., and Eze, P. N.: Soil organic carbon, total nitrogen stocks and CO2 emissions in top-and subsoils with contrasting management regimes in semi-arid environments, Scientific Reports, 13, 1117, 2023.

Poznanović Spahić, M. M., Sakan, S. M., Glavaš-Trbić, B. M., Tančić, P. I., Škrivanj, S. B., Kovačević, J. R., and Manojlović, D. D.: Natural and anthropogenic sources of chromium, nickel and cobalt in soils impacted by agricultural and industrial activity (Vojvodina, Serbia), Journal of Environmental Science and Health, Part A, 54, 219-230, 2019.

Rhoades, J.: Salinity: Electrical conductivity and total dissolved solids, Methods of soil analysis: Part 3 Chemical methods, 5, 417-435, 1996.

Rizwan, M., Ali, S., Qayyum, M. F., Ibrahim, M., Zia-ur-Rehman, M., Abbas, T., and Ok, Y. S.: Mechanisms of biochar-mediated alleviation of toxicity of trace elements in plants: a critical review, Environmental Science and Pollution Research, 23, 2230-2248, 2016.

Sachdeva, S., Kumar, R., Sahoo, P. K., and Nadda, A. K.: Recent advances in biochar amendments for immobilization of heavy metals in an agricultural ecosystem: A systematic review, Environmental Pollution, 319, 120937, 2023.

Saffari, M., Karimian, N., Ronaghi, A., Yasrebi, J., and Ghasemi-Fasaei, R.: Stabilization of nickel in a contaminated calcareous soil amended with low-cost amendments, Journal of soil science and plant nutrition, 15, 896-913, 2015.

Sajadi Tabar, S. and Jalali, M.: Kinetics of Cd release from some contaminated calcareous soils, Natural resources research, 22, 37-44, 2013.

Shahbazi, K., Fathi-Gerdelidani, A., and Marzi, M.: Investigation of the status of heavy metals in soils of Iran: A comprehensive and critical review of reported studies, Iranian Journal of Soil and Water Research, 53, 1163-1212, 10.22059/ijswr.2022.341586.669245, 2022.

Shahbazi, K., Marzi, M., and Rezaei, H.: Heavy metal concentration in the agricultural soils under the different climatic regions: a case study of Iran, Environmental earth sciences, 79, 324, 2020.

Shahzad, B., Tanveer, M., Rehman, A., Cheema, S. A., Fahad, S., Rehman, S., and Sharma, A.: Nickel; whether toxic or essential for plants and environment-A review, Plant Physiology and Biochemistry, 132, 641-651, 2018.

Shen, B., Wang, X., Zhang, Y., Zhang, M., Wang, K., Xie, P., and Ji, H.: The optimum pH and Eh for simultaneously minimizing bioavailable cadmium and arsenic contents in soils under the organic fertilizer application, Science of the Total Environment, 711, 135229, 2020.

Singh, J., Karwasra, S., and Singh, M.: Distribution and forms of copper, iron, manganese, and zinc in calcareous soils of India, Soil Science, 146, 359-366, 1988.

Sparks, D. L., Singh, B., and Siebecker, M. G.: Environmental soil chemistry, Elsevier2022.

Sparrow, L. and Uren, N.: Manganese oxidation and reduction in soils: effects of temperature, water potential, pH and their interactions, Soil Research, 52, 483-494, 2014.

Sumner, M. E. and Miller, W. P.: Cation exchange capacity and exchange coefficients, Methods of soil analysis: Part 3 Chemical methods, 5, 1201-1229, 1996.

Sun, L., Zhang, G., Li, X., Zhang, X., Hang, W., Tang, M., and Gao, Y.: Effects of biochar on the transformation of cadmium fractions in alkaline soil, Heliyon, e12949, 2023.

Sun, Y., Gao, B., Yao, Y., Fang, J., Zhang, M., Zhou, Y., Chen, H., and Yang, L.: Effects of feedstock type, production method, and pyrolysis temperature on biochar and hydrochar properties, Chemical engineering journal, 240, 574-578, 2014.

Tomczyk, A., Sokołowska, Z., and Boguta, P.: Biochar physicochemical properties: pyrolysis temperature and feedstock kind effects, Reviews in Environmental Science and Bio/Technology, 19, 191-215, 2020.

Uchimiya, M., Lima, I. M., Thomas Klasson, K., Chang, S., Wartelle, L. H., and Rodgers, J. E.: Immobilization of heavy metal ions (CuII, CdII, NiII, and PbII) by broiler litter-derived biochars in water and soil, Journal of agricultural and food chemistry, 58, 5538-5544, 2010.

Vickers, N. J.: Animal communication: when i'm calling you, will you answer too?, Current biology, 27, R713-R715, 2017.

Xiao, Z., Peng, M., Mei, Y., Tan, L., and Liang, Y.: Effect of organosilicone and mineral silicon fertilizers on chemical forms of cadmium and lead in soil and their accumulation in rice, Environmental Pollution, 283, 117107, 2021.

Yan, G.-c., Nikolic, M., YE, M.-j., Xiao, Z.-x., and LIANG, Y.-c.: Silicon acquisition and accumulation in plant and its significance for agriculture, Journal of Integrative Agriculture, 17, 2138-2150, 2018.

Yuan, J.-H., Xu, R.-K., and Zhang, H.: The forms of alkalis in the biochar produced from crop residues at different temperatures, Bioresource technology, 102, 3488-3497, 2011.

Zemnukhova, L. A., Panasenko, A. E., Artem'yanov, A. P., and Tsoy, E. A.: Dependence of porosity of amorphous silicon dioxide prepared from rice straw on plant variety, BioResources, 10, 3713-3723, 2015.

Zeng, X., Xiao, Z., Zhang, G., Wang, A., Li, Z., Liu, Y., Wang, H., Zeng, Q., Liang, Y., and Zou, D.: Speciation and bioavailability of heavy metals in pyrolytic biochar of swine and goat manures, Journal of Analytical and Applied Pyrolysis, 132, 82-93, 2018.

Zhao, S.-X., Ta, N., and Wang, X.-D.: Effect of temperature on the structural and physicochemical properties of biochar with apple tree branches as feedstock material, Energies, 10, 1293, 2017.

Zhu, Q., Wu, J., Wang, L., Yang, G., and Zhang, X.: Effect of biochar on heavy metal speciation of paddy soil, Water, Air, & Soil Pollution, 226, 1-10, 2015.